Matrix-Isolation and Mass-Spectrometric Studies of the Thermolysis of $[Me_2N(CH_2)_3]GaMe_2$. Characterization of the Monomeric Organogallanes Me_2GaH, $MeGaH_2$, and MeGa†

Jens Müller,*,‡ Henning Sternkicker,§ Ulf Bergmann,|| and Burak Atakan||

Fakultät für Chemie, Anorganische Chemie II, Ruhr-Universität Bochum, D-44780 Bochum, Germany, Institut für Anorganische Chemie der Technischen Hochschule Aachen, D-52056 Aachen, Germany, and Fakultät für Chemie, Physikalische Chemie I, Universität Bielefeld, D-33501 Bielefeld, Germany

Received: October 26, 1999; In Final Form: January 20, 2000

The thermolysis of the intramolecularly coordinated gallane $[Me_2N(CH_2)_3]GaMe_2$ (**1**) under various conditions has been investigated with matrix-isolation techniques (IR spectroscopy) and with mass spectroscopy (MS). The fragmentation of compound **1** begins above 600 °C; the IR and MS data are in agreement with a proposed β-hydrogen elimination reaction to give allyldimethylamine and dimethylgallane, Me_2GaH. As deduced from the IR spectra of matrix-isolated species, the thermolysis mixtures contain the monomeric gallanes Me_2GaH and $MeGaH_2$, which have been identified with the help of ab initio and DFT calculations. The calculated frequencies [B3LYP/6-311+G(2d,p) and MP2(fc)/6-311+G(2d,p)] are compared with measured IR absorptions. The geometries of Me_2GaH and $MeGaH_2$ have been calculated using several methods [HF, MP2(fc), B3LYP] and basis sets [6-31G(d), 6-311G(d,p), 6-311+G(2d,p)], and the results are discussed and compared with known literature data. Aside from the monomeric hydrides, the argon matrices of the thermolyses experiments contained CH_4, HCN, $H_2C{=}CH_2$, $H_2C{=}C{=}CH_2$, $H_2C{=}NMe$, $[H_2CCHCH_2]^{\bullet}$, $H_2C{=}CHCH_3$, HX, and MeGa. Whereas the carbon-containing species have been identified by comparison with known literature data, methylgallium(I), well-known from mass spectroscopy, was characterized for the first time by IR spectroscopy as a matrix-isolated species. The experimental vibrational frequencies of GaMe are compared with harmonic frequencies calculated at several levels of theory.

Introduction

Group 13 nitrides of Al, Ga, and In are materials with promising applications as new microelectronic and optoelectronic devices.[1,2] In particular, blue-light-emitting diodes and lasers based on gallium nitride can be constructed.[3] Metal organic chemical vapor deposition (MOCVD) of GaN traces its roots to a reaction sequence found by Wiberg[4] for the simple aluminum adduct $Me_3Al{-}NH_3$;[5] that is, GaN is deposited starting from Me_3Ga or Et_3Ga and a large excess of ammonia.[1,2] These triorganogallanes are toxic and very air- and moisture-sensitive, and many attempts were made to synthesize alternative precursors. If the gallium compound is equipped with a ligand that is capable of intramolecular coordination,[6] then non-pyrophoric gallanes are accessible. In particular, the 3-dimethylaminopropyl ligand, $Me_2N(CH_2)_3$, was successfully applied to various gallium precursors; for example, the compound $[Me_2N(CH_2)_3]GaMe_2$ (**1**)[7] can be used as a gallium source in MOCVD processes.[8] A comparable species, but with a built-in nitrogen source, is the diazide $[Me_2N(CH_2)_3]Ga(N_3)_2$; ammonia is not necessary for the MOCVD of GaN from this single-source precursor.[9]

Recently, we began an investigation of the pyrolysis of aluminum[10] and gallium[11] compounds of the type $[Me_2N(CH_2)_3]MX_2$ (X = Cl or Br) using matrix-isolation techniques. Our intent is to trap reactive intermediates produced by the fragmentation of precursors that are equipped with the 3-dimethylaminopropyl ligand. By the characterization of these intermediates, we expect to gain insights into the CVD process. In this paper, we report on our thermolyses experiments with compound **1**. We discuss the results of matrix-isolation IR spectroscopy, mass spectroscopy, and ab initio calculations.

Results and Discussion

Matrix Isolation. We investigated the thermolysis of the intramolecularly coordinated gallium compound $[Me_2N(CH_2)_3]GaMe_2$ (**1**)

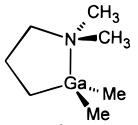

1

with common matrix-isolation techniques; specifically, we used argon as an inert gas and identified matrix-isolated species with IR spectroscopy.

An Al_2O_3 tube that was heated along its last 10 mm was applied for the thermolysis experiments (inner diameter of 1 mm; see Experimental Section). The hot end of the Al_2O_3 tube was only 25 mm away from the cooled matrix window (CsI at 15 K) to ensure that a maximum of volatile fragments emerging from the oven were trapped in argon matrices. With this setup, two different kinds of thermolysis series were carried out: one series with high-vacuum conditions in which a continuous gas flow of the precursor−argon mixture was used and a second

† Part of the special issue "Marilyn Jacox Festschrift".

* E-mail: jens.mueller@aci.ruhr-uni-bochum.de.
‡ Ruhr-Universität Bochum.
§ Technische Hochschule Aachen.
|| Universität Bielefeld.

10.1021/jp9937914 CCC: $19.00
Published on Web 03/10/2000

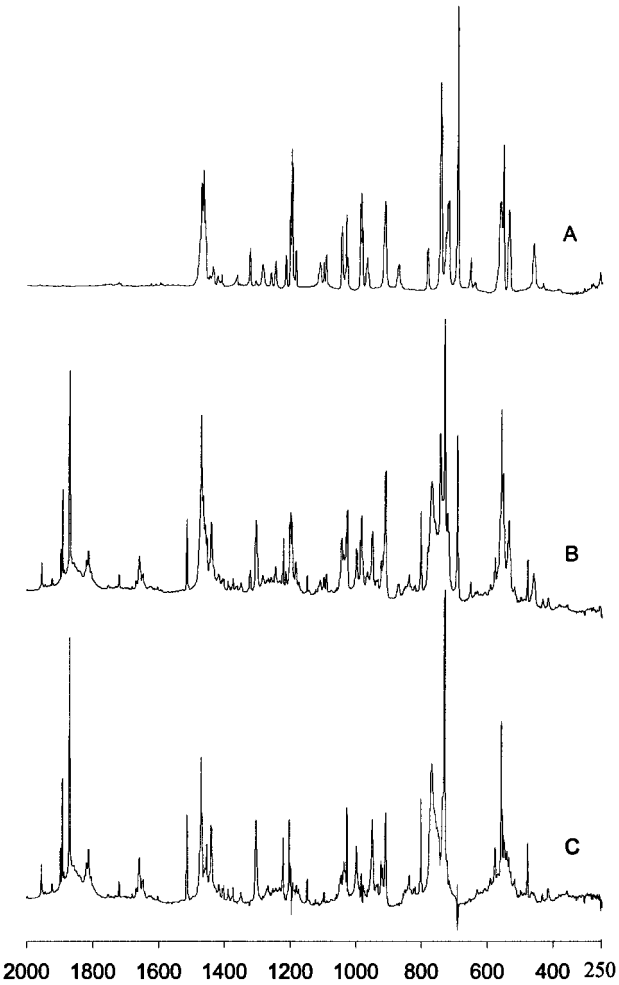

Figure 1. Experimental IR spectra of matrix-isolated species in argon at 15 K. *x* axis, 240−2000 cm^{-1}; *y* axis, absorbance (dimensionless). Spectrum A: starting compound **1**. Spectrum B: results of a pulsed-nozzle thermolysis of compound **1** at ∼1100 °C. Spectrum C: copy of spectrum B from which the absorptions of **1** (spectrum A) have been electronically eliminated. (For assignments, see Tables 1 and 2.).

series in which short pulses of the precursor−argon mixture were conducted through the pyrolysis tube. It is known that, in special cases, the pulsed-nozzle pyrolysis technique is advantageous over the continuous-flow method; for example, Maier et al. showed that some reactive silanes could only be trapped in matrices under pulsed-nozzle thermolysis conditions.[12]

For both thermolysis techniques, the fragmentation of the starting material begins at ∼600 °C. In the case of the continuous-flow thermolyses, the starting compound can no longer be detected if oven temperatures of ∼1000 °C are applied, whereas for the pulsed-nozzle thermolyses, significant amounts of compound **1** are still present in matrices even at oven temperatures of ∼1100 °C. This is illustrated in Figure 1, where trace A is a typical IR spectrum of the matrix-isolated starting compound **1** and trace B is an IR spectrum of the matrix-isolated species produced by a pulsed-nozzle thermolysis at ∼1100 °C. Taking the difference between spectrum B and spectrum A eliminates the absorptions of **1**; hence, the IR bands of spectrum C are due only to products of the thermolysis.

Characterization of Gallium Hydrides. One of the products exhibits an intense IR band at 1869.5 cm^{-1}, which is in the typical region of GaH stretching vibrations. At higher frequencies, two less intense IR bands at 1892.0 and 1898.0 cm^{-1} belonging to a second gallium hydride were measured. The ratio between the two less intense IR bands at the higher frequencies

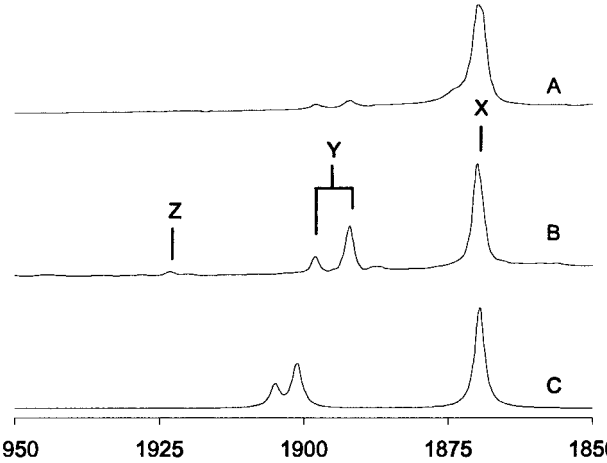

Figure 2. GaH stretching region of matrix-isolated species. *x* axis, 1850−1950 cm^{-1}; *y* axis, absorbance (dimensionless). Spectrum A: results of a continuous-flow thermolysis of **1** at 800 °C. Spectrum B: results of a pulsed-nozzle thermolysis of **1** at 1100 °C (enlargement from Figure 1). X indicates Me_2GaH (1869.5 cm^{-1}), Y indicates $MeGaH_2$ (1898.0 and 1892.0 cm^{-1}), and Z indicates GaH_3 (1923 cm^{-1}). Spectrum C: simulated IR spectrum based on the calculated harmonic frequencies [B3LYP/6-311+G(2d,p) scaled by 0.9786] of Me_2GaH (Table 1) and $MeGaH_2$ (Table 2). A hypothetical mixture with a Me_2GaH:$MeGaH_2$ ratio of 1:0.4 was assumed.

and the intense IR band at 1869.5 cm^{-1} is dependent upon the applied thermolysis conditions. This dependency is illustrated in Figure 2, which compares the GaH stretching regions of IR matrix spectra obtained from a continuous-flow thermolysis (spectrum A) with the corresponding region of a pulsed-nozzle thermolysis (spectrum B). We assigned the intense IR band at 1869.5 cm^{-1} to the GaH stretching mode of monomeric Me_2GaH and the two less intense bands at 1898.0 and 1892.0 cm^{-1} to the symmetric and asymmetric GaH stretching modes of $MeGaH_2$, respectively. In the case of the pulsed-nozzle experiment, we measured a weak IR band at 1923.0 cm^{-1}, which we assigned to the known GaH_3 (Figure 2, spectrum B).[13] The parent gallane, which was very recently synthesized from Ga and H atoms in argon matrices, exhibits three IR absorptions at 1923.2, 758.7, and 717.4 cm^{-1} with an intensity ratio of 1.00:0.70:0.55.[13] In agreement with these data, we measured, in addition to the weak IR band at 1923.0 cm^{-1}, a very weak IR band at 759.0 cm^{-1}. Under continuous-flow thermolysis conditions, there is a tiny band at 1923.0 cm^{-1}, just distinguishable from the baseline, and no absorption at 759.0 cm^{-1}. These facts suggest that the parent gallane is present in the matrices in very low amounts.

In addition to the experimental data, Figure 2 shows the scaled harmonic GaH stretching frequencies for Me_2GaH and $MeGaH_2$ as calculated at the B3LYP/6-311+G(2d,p) level of theory (spectrum C).[14] The complete set of calculated harmonic frequencies at the MP2(fc)/6-311+G(2d,p) and B3LYP/6-311+G(2d,p) levels, together with assignments of measured IR bands, are compiled in Table 1 (Me_2GaH) and Table 2 ($MeGaH_2$). The geometrical parameters calculated at different levels of theory are compiled in Tables 3 and 4, and the molecules are depicted in Figure 3.

Before we discuss the assignments of the measured IR bands to the calculated normal modes, comments on the calculated geometries of the gallium hydrides are necessary. Depending on the calculational methods and the applied basis sets, the ground-state geometry of Me_2GaH exhibits either C_{2v} or C_1 symmetry. This difference is due to an internal torsion of the two methyl groups. The asymmetrical molecules (C_1 point

TABLE 1: Calculated Harmonic Frequencies and Experimental IR Frequencies of Me_2GaH[a]

			MP2(fc)/ 6-311+G(2d,p)	B3LYP/ 6-311+G(2d,p)	experimental frequencies
A_1[b]	ν_1	$\nu_{as}(CH_3)$	3165.9 (20.2)	3107.9 (29.5)	
	ν_2	$\nu_s(CH_3)$	3059.1 (1.9)	3018.4 (2.3)	
	ν_3	ν(GaH)	1955.5 (274.6)	1910.4 (269.1)	1869.5 [0.9560] {0.9786}
	ν_4	$\delta_{as}(CH_3)_{scis}$	1487.9 (1.2)	1461.1 (1.1)	
	ν_5	$\delta_s(CH_3)_{umbr}$	1258.9 (2.8)	1236.7 (1.1)	
	ν_6	$\delta_{as}(CH_3)_{rock}$	779.0 (65.7)	780.8 (63.4)	
	ν_7	$\nu_s(GaC_2)$	550.7 (8.2)	531.0 (6.2)	
	ν_8	$\delta(GaC_2)$	155.9 (4.5)	155.4 (3.7)	
A_2[b]	ν_9	$\nu_{as}(CH_3)$	3138.7 (0.0)	3078.2 (0.0)	
	ν_{10}	$\delta_{as}(CH_3)$	1486.3 (0.0)	1457.9 (0.1)	
	ν_{11}	$\delta_{as}(CH_3)_{twist}$	615.8 (0.0)	610.5 (0.0)	
	ν_{12}	$\tau(CH_3)$	12.4 (0.0)	11.6 (0.0)	
B_1[b]	ν_{13}	$\nu_{as}(CH_3)$	3165.7 (1.2)	3107.3 (1.0)	
	ν_{14}	$\nu_s(CH_3)$	3059.0 (14.6)	3017.5 (19.8)	
	ν_{15}	$\delta_{as}(CH_3)_{scis}$	1479.2 (1.0)	1452.9 (1.9)	
	ν_{16}	$\delta_s(CH_3)_{umbr}$	1256.7 (23.6)	1234.6 (17.6)	1202.5 [0.9569] {0.9740}
	ν_{17}	$\delta_{as}(CH_3)_{rock}$	792.9 (119.2)	785.8 (92.9)	
	ν_{18}	$\nu_{as}(GaC_2)$	590.5 (57.7)	574.1 (38.8)	589.5 [0.9983] {1.0268}[c]
	ν_{19}	δ(CGaH)	554.5 (74.4)	540.4 (85.5)	556.0 [1.0027] {1.0289}
B_2[b]	ν_{20}	$\nu_{as}(CH_3)$	3138.8 (16.7)	3078.8 (24.2)	
	ν_{21}	$\delta_{as}(CH_3)$	1491.0 (3.4)	1462.9 (4.4)	
	ν_{22}	$\delta_{as}(CH_3)_{twist}$	747.3 (77.1)	747.1 (60.7)	729.0 [0.9755] {0.9758}
	ν_{23}	γ(H)	397.5 (48.5)	376.7 (38.3)	415.5 [1.0453] {1.1030}[c]
	ν_{24}	$\tau(CH_3)$	31.2 (0.0)	19.2 (0.1)	

[a] Harmonic frequencies (cm^{-1}) and intensities in parentheses (km mol^{-1}); experimental IR frequencies (cm^{-1}) and observed/calculated frequency ratios in square brackets for MP2 and in braces for B3LYP. [b] Harmonic frequencies are classified assuming C_{2v} symmetry (see Results and Discussion). [c] Tentative assignment.

TABLE 2: Calculated Harmonic Frequencies and Experimental IR Frequencies of $MeGaH_2$[a]

			MP2(fc)/ 6-311+G(2d,p)	B3LYP/ 6-311+G(2d,p)	experimental frequencies
A′[b]	ν_1	$\nu_{as}(CH_3)$	3142.4 (8.9)	3082.3 (12.3)	
	ν_2	$\nu_s(CH_3)$	3060.3 (6.3)	3018.4 (8.4)	
	ν_3	$\nu_s(GaH_2)$	1990.1 (149.1)	1946.6 (147.3)	1898.0 [0.9537] {0.9750}
	ν_4	$\delta_{as}(CH_3)_{scis}$	1491.2 (2.1)	1462.1 (2.7)	
	ν_5	$\delta_s(CH_3)_{umbr}$	1262.8 (11.2)	1238.5 (7.2)	
	ν_6	$\delta_s(GaH_2)_{ip}$	788.2 (205.8)	759.3 (163.9)	
	ν_7	$\delta_{as}(CH_3)_{rock}$	744.3 (129.4)	745.6 (107.0)	
	ν_8	ν(GaC)	579.1 (42.6)	560.5 (37.3)	
	ν_9	$\delta(GaH_2)_{oop}$	514.1 (57.7)	513.4 (39.8)	
A″[b]	ν_{10}	$\nu_{as}(CH_3)$	3171.2 (7.9)	3114.6 (11.2)	
	ν_{11}	$\nu_{as}(GaH_2)$	1978.7 (319.3)	1942.7 (298.1)	1892.0 [0.9562] {0.9739}
	ν_{12}	$\delta_{as}(CH_3)$	1482.5 (1.1)	1455.9 (1.4)	
	ν_{13}	$\delta_{as}(CH_3)_{twist}$	790.7 (75.2)	788.3 (66.8)	
	ν_{14}	$\delta_{as}(GaH_2)_{ip}$	422.5 (37.3)	397.0 (34.8)	
	ν_{15}	$\tau(CH_3)$	14.5 (0.0)	67.4 (0.1)	

[a] Harmonic frequencies (cm^{-1}) and intensities in parentheses (km mol^{-1}); experimental IR frequencies (cm^{-1}) and observed/calculated frequency ratios in square brackets for MP2 and in braces for B3LYP. [b] Harmonic frequencies are classified assuming C_s symmetry (see Results and Discussion).

group) can be approximately described by C_2 point-group symmetries. For example, we optimized the geometry of Me_2GaH at the B3LYP/6-311+G(2d,p) level with the restriction to C_2 symmetry. As judged by the energy, the two slightly different molecules are indistinguishable. At the same DFT level, the C_{2v}-symmetrical species corresponds to a second-order saddle point and is less than 0.004 kJ mol^{-1} higher in energy than the ground state. For comparison, Bock and Mains et al. found a C_{2v}-symmetrical ground-state geometry for Me_2GaH at the HF/HUZSP* level of theory (see Table 3) and a rotational barrier for the methyl groups of less than 0.1 kJ mol^{-1}.[15] This result suggests that the true barrier for the methyl-group rotation is extremely low. Obviously, the flatness of the potential energy surface with respect to methyl-group rotation makes the determination of the true minimum structure by theory difficult. On the other hand, because this barrier is so low, the harmonic

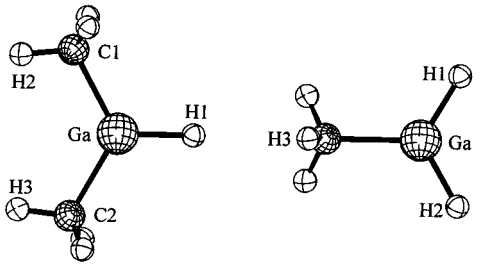

Figure 3. Calculated ground-state geometries of Me_2GaH and $MeGaH_2$. Depicted are the MP2(fc)/6-311+G(2d,p) results.

frequencies (of course, except for those of the torsion motions of the methyl groups) are not influenced by the conformations of the methyl groups. Therefore, we describe the harmonic frequencies of Me_2GaH in Table 1 as if the ground-state geometry were C_{2v}-symmetrical; that is, the 24 normal modes of Me_2GaH transform according to the irreducible representations A_1 (8), A_2 (4), B_1 (7), and B_2 (5). Comparable results are obtained for $MeGaH_2$; the HF and MP2 methods give C_s-symmetrical minimum geometries, whereas the B3LYP method results in geometries with a different conformation of the methyl group (C_1 symmetry; Figure 3 and Table 4). The harmonic frequencies of $MeGaH_2$ in Table 2 are described according to a C_s-symmetrical geometry.

For Me_2GaH, we could assign six experimental IR bands to calculated normal modes (Table 1). Under various thermolysis conditions, these absorptions increase or decrease relative to the other IR bands. The ratios between measured and calculated IR frequencies are typical with respect to the applied theoretical levels.[16] The B3LYP frequency of a particular vibration is lower than the MP2 frequency, and the low-frequency modes are underestimated by the B3LYP method, resulting in observed/calculated ratios that are larger than 1.[17] The highest observed/calculated ratios of 1.0453 (MP2) and 1.1030 (B3LYP) are found for the out-of-plane hydrogen vibration ν_{23}; similar values have been obtained for the gallium hydrides Cl_2GaH and Br_2GaH.[11] However, some of the normal modes, predicted to cause IR absorptions intense enough to be detectable, could not be assigned, namely, the CH stretching modes ν_1, ν_{14}, and ν_{20} and the CH_3 rocking modes ν_6 and ν_{17}. The matrices always contain many species equipped with methyl groups, such as starting compound **1**, Me_2GaH, $MeGaH_2$, and others (see below), that exhibit many similar vibrational modes (Figure 1). Thus, it is impossible to assign one of the CH stretching modes with certainty. The same difficulty seems to hold for the rocking modes ν_6 and ν_{17}, with calculated wavenumbers in the range of 779−793 cm^{-1} (Table 1). We assume that these two modes contribute to a broad, unresolved IR band at 768 cm^{-1}, which is present in every IR spectrum of the thermolysis products. Additional contributions to the unresolved absorption at 768 cm^{-1} might come from the vibrational modes ν_6, ν_7, and ν_{13} of $MeGaH_2$ (Table 2).

For $MeGaH_2$, the symmetrical and asymmetrical GaH stretching vibrations, ν_3 and ν_{11}, are the only modes that could be assigned with certainty. This certainty is based on the fact that the observed/calculated ratios obtained for these modes are similar to the ratio found for the GaH stretch ν_3 of Me_2GaH (Tables 1 and 2). Furthermore, the calculated intensities match quite nicely with the measured intensities (Figure 2). Because the relative amount of $MeGaH_2$ in the matrices is low, additional normal modes could not be assigned.

Mechanistic Considerations. The first step of the thermolysis of compound **1** is quite probably a β-hydrogen elimination reaction (eq 1).

TABLE 3: Selected Bond Lengths (Å), Angles (deg), and Torsional Angles (deg) of Me_2GaH

		d(Ga−H1)	*d*(Ga−C1)	*d*(Ga−C2)	H1−Ga−C1	H1−Ga−C2	C−Ga−C	H1−Ga−C1−H2	H1−Ga−C2−H3
HF									
6-31G(d)	C_1	1.583	1.990	1.990	119.26	119.27	121.48	−154.38	−154.08
6-311G(d,p)	C_{2v}	1.584	1.990	1.990	118.52	118.52	122.97	180.00	180.00
6-311+G(2d,p)	C_{2v}	1.585	1.989	1.989	118.48	118.48	123.05	180.00	180.00
HUZSP*[a]	C_{2v}	1.592	1.994	1.994	118.55	118.55	122.90	180.00	180.00
B3LYP									
6-31G(d)	C_1	1.580	1.984	1.984	118.63	118.64	122.74	−168.30	−167.91
6-311G(d,p)	C_1	1.579	1.985	1.985	118.47	118.46	123.06	−175.42	−175.82
6-311+G(2d,p)	C_1	1.579	1.984	1.984	118.47	118.47	123.06	−177.44	−177.48
MP2(fc)									
6-31G(d)	C_1	1.595	1.992	1.992	119.18	119.27	121.56	−159.62	−157.40
6-311G(d,p)	C_1	1.585	1.994	1.994	118.94	118.94	122.12	−173.88	−173.85
6-311+G(2d,p)[b]	C_1	1.587	1.997	1.997	118.85	118.85	122.30	180.00	180.00

[a] Data from ref 15. [b] Approximately C_{2v} symmetry.

TABLE 4: Selected Bond Lengths (Å), Angles (deg), and Torsional Angles (deg) of $MeGaH_2$

		d(Ga−H1)	*d*(Ga−H2)	*d*(Ga−C)	H1−Ga−C	H2−Ga−C	H−Ga−H	H1−Ga−C−H3[b]
HF								
6-31G(d)	C_s	1.578	1.578	1.985	121.16	121.16	117.67	89.48
6-311G(d,p)	C_s	1.578	1.578	1.986	120.69	120.69	118.60	89.43
6-311+G(2d,p)	C_s	1.579	1.579	1.985	120.72	120.72	118.55	89.46
HUZSP*[a]	C_s	1.586	1.586	1.991	—[c]	—[c]	118.75	—[c]
B3LYP								
6-31G(d)	C_1	1.574	1.574	1.978	120.55	121.79	117.66	76.29
6-311G(d,p)	C_1	1.572	1.572	1.981	120.08	121.17	118.74	77.93
6-311+G(2d,p)	C_1	1.572	1.572	1.979	120.12	121.13	118.74	78.23
MP2(fc)								
6-31G(d)	C_s	1.589	1.589	1.987	121.02	121.02	117.95	89.19
6-311G(d,p)	C_s	1.579	1.579	1.990	120.39	120.39	119.20	89.31
6-311+G(2d,p)	C_s	1.580	1.580	1.993	120.22	120.22	119.56	89.46

[a] Data from ref 15. [b] For the C_s-symmetrical species, the torsion angle H1GaCH3 is not equal to 90.00° because of a weakly pyramidal configuration at the Ga atom. [c] Values not given in ref 15.

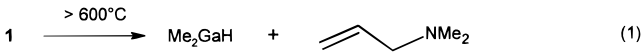

(1)

In accord with eq 1, we identified allyldimethylamine among the thermolysis products.[18]

We suspect that the dihydride $MeGaH_2$ is formed through a ligand-exchange gas-phase reaction according to eq 2.

(2)

In agreement with eq 2, Me_3Ga was unambiguously identified by comparison with known literature data.[19] As mentioned before, the $MeGaH_2$ to Me_2GaH ratio is dependent upon the thermolysis conditions. The relative amount of $MeGaH_2$ is higher under pulsed-nozzle thermolysis conditions, and the same applies for Me_3Ga, which supports the proposed gas-phase exchange reaction (eq 2).

The parent gallane, GaH_3, might be formed in the gas phase by a ligand-exchange reaction starting from $MeGaH_2$, a ligand exchange that is similar to eq 2. However, it is possible that GaH_3 is formed in argon matrices from H and Ga atoms, which could be produced by the thermolysis of the precursor **1**. So far, neither of the two reaction paths to GaH_3 can be ruled out on the basis of the experimental evidence. However, the amounts of hydrides decrease in the order Me_2GaH, $MeGaH_2$, and GaH_3 (Figure 2). This ordering agrees with the suggested ligand-exchange reactions: a fraction of Me_2GaH, the product of the β-hydrogen elimination, gives the dihydride $MeGaH_2$ (eq 2), and a fraction of this species could give GaH_3 via a further ligand-exchange reaction in the gas phase.

Additional Products. As mentioned in the Introduction, we recently investigated the thermolyses of intramolecularly coordinated chlorides and bromides of the type $[Me_2N(CH_2)_3]MX_2$ (M = Al or Ga, and X = Cl or Br).[10,11] In all cases, we identified the monomeric hydrides HMX_2, the M(I) species MX, and the known products CH_4, HCN, $H_2C{=}CH_2$, $H_2C{=}NMe$, $[H_2CCH_2\text{-}CH_2]^{\bullet}$, and $H_2C{=}CHCH_3$. The same carbon-containing compounds are formed by the pyrolyses of compound **1**, and in addition, $H_2C{=}C{=}CH_2$ can be identified by its IR bands at 1955.0 and 837.0 cm^{-1}.[20]

Furthermore, we identified methylgallium(I), MeGa, in argon matrices (Table 5). As can be seen from calculated data in Table 5, the nine normal modes of this C_{3v}-symmetrical species should result in six IR bands. We assigned the CH_3 deformation mode ν_2 and the GaC stretching mode ν_3 to the measured IR bands at 1148.5 and 476.5 cm^{-1}, respectively. As predicted by theory, the GaC stretching mode ν_3 is more intense than the deformation mode ν_2. Two of the remaining four modes are the CH stretching modes ν_1 and ν_4, which cannot be assigned for the reasons already discussed above. Of the remaining two modes, ν_5 and ν_6, the latter should result in the least intense IR resonance, and we assume that the intensity is not high enough to be observable under our experimental conditions. According to calculations at several levels of theory (Table 5), the asymmetric CH_3 deformation mode ν_5 results in an IR band of intensity comparable to that of the measured transition ν_2 (1148.5 cm^{-1}). However, we could not assign the mode ν_5 because, in the expected region around 1400 cm^{-1}, there are too many IR bands; only the two IR absorptions at 1148.5 and 476.5 cm^{-1} are nicely separated from other IR absorptions and, thus, can be assigned with certainty to ν_2 and ν_3 of MeGa, respectively.

Methylgallium(I) is well-known in the gas phase by mass spectrometry; it is an important intermediate in the fragmentation paths of Me_3Ga in CVD processes.[23] Independent from our investigations, MeGa was very recently synthesized photo-

TABLE 5: Calculated Harmonic Frequencies and Experimental IR Frequencies of MeGa (C_{3v})

	A_1			E^d		
	ν_1 [$\nu_s(CH_3)$]	ν_2 [$\delta_s(CH_3)$]	ν_3 [ν(GaC)]	ν_4 [$\nu_{as}(CH_3)$]	ν_5 [$\delta_{as}(CH_3)_{scis}$]	ν_6 [$\delta_{as}(CH_3)_{rock}$]
exp. frequencies		1148.5	476.5			
MP2(fc)/6-311+G(2d,p)[a]	3023.6 (14.6)	1209.3 (29.0) [0.9497]	495.8 (84.4) [0.9611]	3119.3 (15.0)	1462.2 (14.2)	502.5 (6.9)
B3LYP/6-311+G(2d,p)[a]	2978.7 (19.9)	1183.2 (23.5) [0.9707]	477.6 (78.9) [0.9977]	3053.4 (24.6)	1434.7 (12.9)	488.7 (4.5)
B3P86/6-311G(3df,3pd)[b]	3002.0 (12.1)	1175.0 (19.1) [0.9774]	493.0 (78.2) [0.9665]	3088.0 (18.0)	1424.0 (10.4)	479.0 (3.2)
B3PW91/6-311G(3df,3pd)[b]	2994.0 (18.8)	1179.0 (17.7) [0.9741]	494.0 (77.7) [0.9646]	3078.0 (18.8)	1424.0 (10.3)	485.0 (3.6)
B3LYP/6-311G(3df,3pd)[b]	2984.0 (17.0)	1188.0 (13.6) [0.9668]	479.0 (76.5) [0.9948]	3059.0 (23.8)	1434.0 (9.3)	483.0 (4.7)
CISD/TZP[c]	3059.7 (18.0)	1245.2 (21.5) [0.9223]	508.9 (76.1) [0.9363]	3149.6 (24.8)	1484.8 (11.4)	512.9 (7.6)
CCSD(T)/TZP[c]	2983.4 (17.9)	1204.2 (15.2) [0.9537]	496.3 (68.0) [0.9601]	3076.2 (23.8)	1444.2 (10.6)	497.1 (6.9)

[a] This work. [b] Data from ref 21. [c] Data from ref 22. [d] The intensities of only one vibration of the E modes are listed.

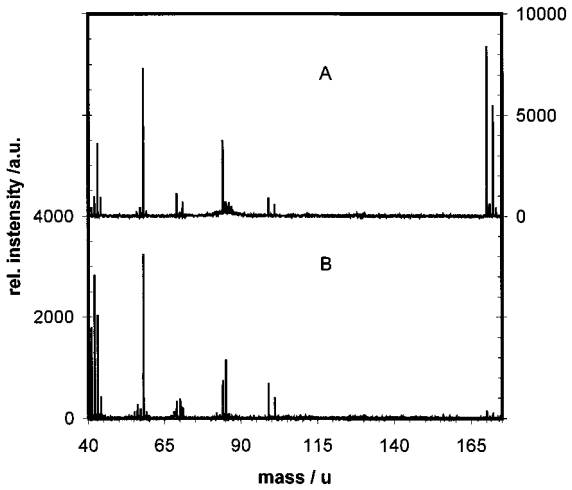

Figure 4. Mass spectra of **1** measured at 23 °C (spectrum A) and 750 °C (spectrum B). The signals at 58 and 43 u are due to residues of acetone in the ionization chamber.

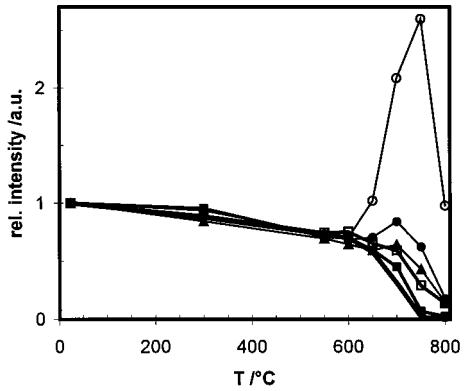

Figure 5. Temperature dependence of some mass-spectrometric signals, normalized to their values at room temperature. □, 69.95/71.95 u; ▲, 83.95/85.95 u; ■, 84.95/86.95 u; ○, 85.1 u; ●, 98.95/100.95 u; and solid line, 169.95/171.95 u.

chemically from Ga atoms and CH_4 in argon matrices and was characterized by IR spectroscopy.[24]

Mass-Spectrometric Investigations. Parallel to the matrix-isolation experiments, we investigated the thermolysis of compound **1** by mass spectroscopy using a resistively heatable quartz tube (inner diameter of 4 mm; heated zone of 100 mm; see Experimental Section). Mass spectra were measured between ambient temperature and 800 °C, with applied ionization energies of 15 and 35 eV for electron impact. These two different energies represent a tradeoff between high sensitivity and low fragmentation. At 35 eV, the sensitivity is much higher than at 15 eV, but the extent of fragmentation is greater. This is especially true for organogallium compounds because of their low ionization potentials. However, because of the increased sensitivity at 35 eV, indications of gallium-containing gas-phase compounds could be derived from these spectra even if these compounds were present in small amounts. Two typical mass spectra are shown in Figure 4. Spectrum A, which was measured at ambient temperature, shows the fragmentation pattern of compound **1** caused by ionization. The base peak appears at 169.95/171.95 u ($\mathbf{1}^+ - CH_3$) with further fragments at 98.95/100.95 (Me_2Ga^+), 84.1 ($C_5H_{10}N^+$), and 68.95/70.95 u (Ga^+). Trace B of Figure 4 shows the results of the thermolysis of **1** at 750 °C. The most prominent difference between the two spectra is a lack of the signal at 169.95/171.95 u ($M^+ - CH_3$) in spectrum B. However, in both spectra the signal at 98.95/100.95 u (Me_2Ga^+) is present with comparable intensity; hence, for spectrum B, this signal must originate from thermolysis products of compound **1**. The high intensity of the signal at 98.95/100.95 u suggests that this signal is caused by a primary thermolysis product, and it is probably mainly attributable to dimethylgallane, Me_2GaH. That the molecular ion of Me_2GaH was not detected is not surprising; for example, 98.95/100.95 u (Me_2Ga^+) is the most prominent signal in mass spectra of trimethylgallium.[25,26]

The relative intensities of selected signals as a function of temperature are shown in Figure 5. For a better comparison of the data, all signals in Figure 5 are normalized to their values at ambient temperature; however, the absolute intensities of the signals differ greatly. It can be seen from Figure 5 that the pyrolysis of compound **1** begins above 600 °C and is completed at 750 °C; at this temperature, the signal at 169.95/171.95 u ($\mathbf{1}^+ - CH_3$) is below the detection limit. That, indeed, pyrolysis of **1** takes place can be illustrated with the signal at 85.05 u. Up to 600 °C, this signal shows a behavior similar to the signal at 169.95/171.95 u ($\mathbf{1}^+ - CH_3$), and above 600 °C, its intensity increases greatly. The signal at 85.05 u corresponds to the formula $C_5H_{11}N^+$, which we interpret as the cation of allyldimethylamine. So far, these data support the proposed β-hydrogen elimination of eq 1. An alternative to the β-hydrogen elimination pathway is a fragmentation of **1** into $Me_2Ga^\bullet$ and $(CH_2)_3NMe_2^\bullet$ radicals. These radicals might further react with hydrogen sources, which would lead to the saturated amine $H_3C(CH_2)_2NMe_2$. The $(CH_2)_3NMe_2^\bullet$ radical and the saturated amine correspond to signals at 86.05 and 87.05 u, respectively, but the signals for these masses showed the same behavior as the signals at 169.95/171.95 u.

Other signals of gallium-containing compounds and fragments were found at 68.95/70.95 (Ga^+), 98.95/100.95 (Me_2Ga^+), and 83.95/85.95 u ($MeGa^+$). These signals show a behavior that is, up to 600 °C, similar to the behavior of the signal at 169.95/171.95 u, so it can be assumed that these signals in the lower temperature range are due solely to the fragmentation of **1**. At temperatures above 650 °C, these signals do not drop in a manner parallel to that of the signal at 169.95/171.95 u, but rather, they remain at a higher level. Consequently, they should

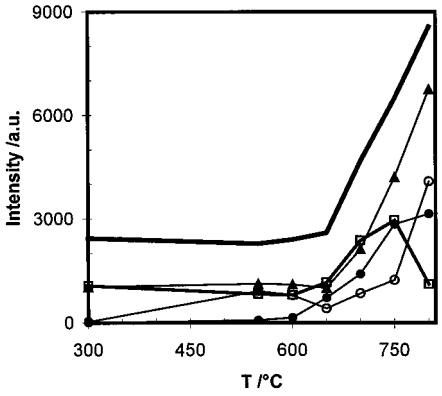

Figure 6. Temperature dependence of some mass-spectrometric signals. Only the temperature range above 300 °C is shown, because only negligible changes can be found at lower temperatures. ●, 16 u; ○, 27 u; ▲, 41 u; solid line, 42 u; and □, 85.1 u.

have a different source, namely, some other gallium-containing gas-phase compounds. In accordance with the matrix-isolation studies, the signal at 98.95/100.95 u (Me_2Ga^+) above 600 °C should be mainly due to fragmentation of Me_2GaH and Me_3Ga. The difference between the signal groups at 83.95/85.95 u ($MeGa^+$) and 169.95/171.95 u above 600 °C is small, but this difference could be indicative of the fragmentation of gas-phase hydrides such as Me_2GaH or $MeGaH_2$. At temperatures above 750 °C, all of the signals of gallium-containing gas-phase compounds drop below the detection limit, probably as a result of the formation of liquid gallium at the reactor walls.

Furthermore, several low-mass compounds could be detected. The temperature dependence of the signals corresponding to these compounds is shown in Figure 6 for the temperature range of 300−800 °C. Their signals obviously increase at higher temperatures so that normalization is not necessary. Methane (16 u) is formed at temperatures above 600 °C. It could be produced by the reaction of methyl radicals with **1** or with other hydrogen sources, but reactions such as the fragmentation of Me_2GaH and $MeGaH_2$ into methane and MeGa are also feasible. The signal at 27 u unequivocally shows the presence of HCN, and higher temperatures appear to favor the formation of HCN. In particular, there is a significant increase in the intensity of the signal at 27 u (HCN^+) from 750 to 800 °C, whereas the intensity of the signal at 85.1 u ($C_5H_{11}N^+$) decreases. This suggests that HCN is formed via pyrolysis of allyldimethylamine at high temperature. At 28 u, the strong signal of the buffer-gas nitrogen prevents the detection of ethylene. Additional signals are found at 41, 42, and 43 u, and all three signals increase greatly above 600 °C; two of these signals are included in Figure 6. The peaks at 43 and 42 u could be due to CH_3NCH_2 and perhaps its fragmentation product C_2H_4N, but C_3H_6 might also be the source of the signal at 42 u. The signals at 41, 42, and 43 u show the same temperature dependence above 600 °C when the lower ionization energy of only 15 eV is applied; hence, the influence of fragmentation is not important.

Conclusion

The combination of matrix-isolation and mass-spectroscopic techniques reveals a conclusive picture of the thermolysis of the gallium precursor **1**. Above 600 °C, β-hydrogen elimination to allyldimethylamine and dimethylgallane occurs (eq 1). With increasing temperature, smaller carbon-containing fragments become more prominent, whereas the amount of allyldimethylamine decreases. It is known that organogallanes can undergo β-hydrogen eliminations. For example, Russell et al. investigated intensively the fragmentation of trialkylgallanes with the infrared laser-powered homogeneous pyrolysis (IR LPHP) technique.[27] With this method, Et_3Ga was thermolyzed to give either $(Et_2GaH)_x$ or $(EtGaH_2)_x$ and ethane. The pure hydrides, as well as their NMe_3 adducts, were identified by FTIR and NMR spectroscopy. The gallanes are oligomers; however, monomeric species were not detected. Furthermore, ab initio calculations have suggested that the β-hydrogen elimination route has a lower activation barrier than the alternative homolysis pathway for simple gallanes.[28]

Monomeric gallium hydrides with 3-fold-coordinated Ga atoms are rare.[29] To date, only a few compounds of this type have been characterized, namely, Cl_2GaH,[30] Br_2GaH,[11] $ClGaH_2$,[31] and GaH_3[13] in rare-gas matrices by IR spectroscopy and the sterically crowded compounds Mes^*_2GaH,[32] Mes^*GaH_2,[33] and $Mes^*(3,5\text{-}t\text{Bu}_2C_6H_3CMe_2CH_2)GaH$[33] ($Mes^* = 2,4,6\text{-}t\text{Bu}_3C_6H_2$) by single-crystal X-ray determination.

The structure of dimethylgallane as a bulk material is unknown. However, on the basis of gas-phase electron-diffraction experiments, the vapor phase of this hydride is thought to consist of the dimers $Me_2Ga(\mu\text{-}H)_2GaMe_2$.[34] Other well-known hydrides of the same type are $H_2Ga(\mu\text{-}H)_2GaH_2$,[35] $H_2Ga(\mu\text{-}Cl)_2GaH_2$,[36] $H_2Ga(\mu\text{-}NMe_2)_2GaH_2$,[37] and $Me_2Ga(\mu\text{-}Cl)_2GaMe_2$.[34] In the course of the investigation on the structure of gaseous dimethylgallane, Downs et al. measured the IR spectra of the $(Me_2GaH)_n$ vapor isolated in argon matrices.[34] The spectra could be interpreted satisfactorily by assuming the presence of the dimeric species $Me_2Ga(\mu\text{-}H)_2GaMe_2$. In addition to the main absorptions, IR bands of weak but variable intensity in the region of 1850−2000 cm^{-1} were attributed to impurities, Lewis acid−base adducts of the type $Me_2GaH{-}B$ such as $Me_2GaH{-}OH_2$. The most intense absorption in that region was found at 1870 cm^{-1} as a sharp IR band. Recent studies with Ga_2H_6 raised the possibility that this IR band is actually due to the Me_2GaH monomer.[38] Within the experimental error, the absorption at 1870 cm^{-1} matches our IR band at 1869.5 cm^{-1}, which we unequivocally assigned to the GaH stretching mode of monomeric Me_2GaH.

With the characterization of Me_2GaH and $MeGaH_2$, we have shown that monomeric organometallic gallium hydrides can be obtained by a high-temperature reaction path.

Experimental Section

General Remarks. All synthetic procedures were carried out under dry nitrogen atmospheres with standard Schlenk techniques. Solvents were dried by standard procedures, distilled, and stored under nitrogen and molecular sieves (4 Å). Compound **1** was prepared according to the literature procedure.[7b]

Matrix Isolation. The matrix apparatus consisted of a vacuum line (Leybold Turbovac 151; Leybold Trivac D4B) and a Displex CSW 202 cryogenic closed-cycle system (APD Cryogenics Inc.) fitted with CsI windows. For the experiments using the pulsed-nozzle pyrolysis technique, compound **1** was kept in a small, metal container that was connected to the matrix apparatus via a pulse valve (Pulse Valve Series 9, IOTA One, General Valve Corporation; opening diameter of 0.8 mm). In a typical experiment, **1** was kept under an argon pressure of 2 bar (Linde 6.0) and heated to 55 °C. Pulses of 500 μs at 10 Hz were passed through an Al_2O_3 tube (inner diameter of 1 mm; heated by tungsten wire coiled around the last 10 mm). The hot end of the pyrolysis tube was just 25 mm away from the cooled CsI window to ensure that a maximum amount of the volatile fragments emerging from the oven was trapped in matrices (CsI at 20 K). For the temperature determination of

the pyrolysis oven, a current-to-temperature relationship was measured with a thermocouple (Thermocoax; NiCr/NiAl) placed inside the Al_2O_3 tube. For the experiments using the continuous-flow technique, compound **1** was kept in the small, metal container under high vacuum (10^{-6} to 10^{-7} mbar) at constant temperature (−14 °C) while a flow of argon was conducted over the sample (Linde 6.0; flow = 1.0 sccm; MKS mass-flow controller type 1179). The gaseous mixture passed through an Al_2O_3 tube with two parallel, inner canals (outer diameter of 4 mm; inner diameter of 1 mm each; last 10 mm heated with a tungsten wire) and with one of the inner canals equipped with a thermocouple (Thermocoax; NiCrSi/NiSi). With this setup, it is possible to measure reliable thermolysis temperatures without a contact between the substance and the thermocouple. The gaseous mixtures were trapped onto the CsI window at 15 K.

The concentrations of the samples in the matrices were unknown. Therefore, several experiments under various conditions were performed to guarantee that the molecules were indeed matrix-isolated. The concentration of the samples decreased significantly at lower sample temperatures, but no differences in the IR spectra were observed. At higher concentrations, the half bandwidths of the IR bands increased, and new, broad IR bands appeared, indicating that notable parts of the molecule were no longer matrix-isolated under these conditions.

The IR spectra of the matrices (at 15 K for the continuous technique and at 20 K for the pulsed-nozzle technique) were recorded on a Perkin-Elmer FTIR 1720x spectrometer from 240 to 4000 cm^{-1} with a resolution of 1 cm^{-1}.

Ab Initio Calculations. The Gaussian 94 package,[14] run on a cluster of workstations (Rechenzentrum der RWTH Aachen), was employed for all calculations. The total energies E_h (in hartree) and the zero-point vibrational energy (in kJ mol^{-1}; in parentheses), followed by the calculational method and the ground-state symmetry (in parentheses), are as follows.

Me_2GaH: −2001.0279131 (215.97) for HF/6-31G(d) (C_1); −2003.0273835 (212.89) for HF/6-311G(d,p) (C_{2v}); −2003.0297609 (212.67) for HF/6-311+G(2d,p) (C_{2v}); −2003.3499920 (204.75) for B3LYP/6-31G(d) (C_1); −2005.3148651 (202.23) for B3LYP/6-311G(d,p) (C_1); −2005.3148646 (201.93) for B3LYP/6-311G(d,p) (C_{2v}); −2005.3163782 (201.91) for B3LYP/6-311+G(2d,p) (C_1); −2005.3163768 (201.73) for B3LYP/6-311+G(2d,p) (C_{2v}) −2001.3449165 (208.95) for MP2(fc)/6-31G(d) (C_1); −2003.4109712 (205.77) for MP2(fc)/6-311G(d,p) (C_1); −2003.4109709 (205.69) for MP2(fc)/6-311G(d,p) (C_{2v}); −2003.4305434 (205.58) for MP2(fc)/6-311+G(2d,p) (C_1).

$MeGaH_2$: −1961.9803283 (133.96) for HF/6-31G(d) (C_s); −1963.9741368 (132.43) for HF/6-311G(d,p) (C_s); −1963.9741086 (132.18) for HF/6-311+G(2d,p) (C_s); −1964.0214059 (127.44) for B3LYP/6-31G(d) (C_1); −1965.9780509 (126.25) for B3LYP/6-311G(d,p) (C_1); −1965.9776116 (126.16) for B3LYP/6-311+G(2d,p) (C_1); −1962.1652130 (129.62) for MP2(fc)/6-31G(d) (C_s); −1964.2051909 (128.33) for MP2(fc)/6-311G(d,p) (C_s); −1964.2143385 (128.20) for MP2(fc)/6-311+G(2d,p) (C_s).

MeGa: −1964.7751117 (87.29) for B3LYP/6-311+G(2d,p) (C_{3v}); −1963.0267516 (89.10) for MP2(fc)/6-311+G(2d,p) (C_{3v}).

Mass-Spectrometric Investigations. The experiment will be described briefly, as additional details can be found in refs 25 and 39. The reaction was studied with a resistively heatable quartz tube (inner diameter of 4 mm; heated zone of 100 mm). The accessible temperature range was 293−1300 K, as measured by Ni/CrNi thermocouples outside the tube; these thermocouples were calibrated in separate measurements against thermocouples inside the tube under similar gas-flow conditions. The typical pressure inside the reactor was 10 mbar, as measured by absolute pressure transducers (Balzers; compact full-range gauge). A quartz nozzle with an inner diameter of 0.25 mm was used to probe the gas mixture at the end of the quartz tube reactor. Behind the quartz nozzle, the pressure was reduced to $<10^{-3}$ mbar by an oil diffusion pump (Varian; VHS-6; 3000 L/s), so that a molecular beam was formed. With this setup, additional collisions were efficiently avoided, and the composition of the reaction mixture was "frozen". Behind a copper skimmer with an aperture (diameter of 0.8 mm), the ionization chamber was situated; in that region, the pressure was reduced below 2×10^{-5} mbar by a turbo-molecular pump (Balzers; TMH 260).

The gas mixture was analyzed by a time-of-flight mass spectrometer (mass range ≤500 u) equipped with a reflectron (Käsdorf). The mass resolution of $m/\Delta m = 3000$ was sufficient to resolve gallium-containing compounds from hydrocarbons with comparable masses (for example, 84.95 and 85.1). The applied ionization energy in the electron-impact experiments always represented a tradeoff between high sensitivity and low fragmentation, so that the experiments were performed at both 15 and 35 eV. The electron beam was typically pulsed at 10 kHz, and the ions for each flight time were counted, typically for 10^6 pulses. To reduce the effect of long-time changes in the sensitivity, the signal counts were always normalized to the signal of the internal standard argon. At each temperature, a background spectrum was recorded and subtracted from the data to avoid misinterpretations. The gas flows of nitrogen and argon were regulated by calibrated mass-flow controllers (Tylan). Argon was passed through an actively cooled (typically to 5 °C) saturator equipped with compound **1**. The gases (N_2, 5.0; Ar, 4.5) were further purified by conducting them through an oxygen and water absorber (Oxisorb; Messer). The total mass-flow rate was fixed at 20 sccm, resulting in reaction times of approximately 40 ms.

Acknowledgment. This work was supported by the Fonds der Chemischen Industrie, the Deutsche Forschungsgemeinschaft, and the Wissenschaftsministerium of Nordrhein-Westfalen (Bennigsen-Foerder Preis, B.A.). We thank Prof. K. Kohse-Höinghaus for her continuous support of this work and for many helpful discussions. We are grateful to the Rechenzentrum der RWTH Aachen for providing generous computer time; in particular, we thank T. Eifert and J. Risch for their support. We also thank P. Geisler (RWTH Aachen) for the construction of the thermolysis oven for the matrix-isolation experiments.

References and Notes

(1) Neumayer, D. A.; Ekerdt, J. G. *Chem. Mater.* **1996**, *8*, 9 and references therein.

(2) Jones, A. C.; O'Brien, P. *CVD of Compound Semiconductors*; VCH Publishers: Weinheim, Germany, 1997.

(3) Nakamura, S.; Fasol, G. *The Blue Laser Diode, GaN Based Light Emitters and Lasers*; Springer Publishing: New York, 1997.

(4) Bähr, G. In *FIAT Review of WWII German Science, 1939−1946. Inorganic Chemistry, Part II*; Klemm, W., Ed.; Dieterichsche Verlagsbuchhandlung: Wiesbaden, Germany, 1948; p 155.

(5) Müller, J.; Ruschewitz, U.; Indris, O.; Hartwig, H.; Stahl, W. *J. Am. Chem. Soc.* **1999**, *121*, 4647 and references therein.

(6) Gruter, G.-J. M.; van Klink, G. P. M.; Akkerman, O. S.; Bickelhaupt, F. *Chem. Rev.* **1995**, *95*, 2405.

(7) (a) Schumann, H.; Hartmann, U.; Dietrich, A.; Pickardt, J. *Angew. Chem.* **1988**, *100*, 1119; *Angew. Chem., Int. Ed. Engl.* **1988**, *27*, 1077. (b) Schumann, H.; Hartmann, U.; Wassermann, W. *Polyhedron* **1990**, *9*, 353.

(8) Erdmann, D.; van Ghemen, M. E.; Pohl, L.; Schumann, H.; Hartmann, U.; Wassermann, W.; Heyen, M.; Jürgensen, H. Metallorganische Verbindungen. Patent DE 3631469 A1, 1988; *Chem. Abstr.* **1988**, *109*, 42300.

(9) (a) Miehr, A.; Mattner, M. R.; Fischer, R. A. *Organometallics* **1996**, *15*, 2053. (b) Miehr, A.; Ambacher, O.; Rieger, W.; Metzger, T.; Born, E.; Fischer, R. A. *Chem. Vap. Deposition* **1996**, *2*, 51. (c) Fischer, R. A.; Miehr, A.; Herdtweck, E.; Mattner, M. R.; Ambacher, O.; Metzger, T.; Born, E.; Weinkauf, S.; Pulham, C. R.; Parsons, S. *Chem.*−*Eur. J.* **1996**, *2*, 1353.

(10) Müller, J.; Wittig, B. *Eur. J. Inorg. Chem.* **1998**, 1807.

(11) Müller, J.; Sternkicker, H. *J. Chem. Soc., Dalton Trans.* **1999**, 4149.

(12) Maier, G.; Reisenauer, H. P.; Pacl, H. *Angew. Chem.* **1994**, *106*, 1347; *Angew. Chem., Int. Ed. Engl.* **1994**, *33*, 1248.

(13) Pullumbi, P.; Bouteiller, Y.; Manceron, L.; Mijoule, C. *Chem. Phys.* **1994**, *185*, 25.

(14) Frisch, M. J.; Trucks, G. W.; Schlegel, H. B.; Gill, P. M. W.; Johnson, B. G.; Robb, M. A.; Cheeseman, J. R.; Keith, T.; Petersson, G. A.; Montgomery, J. A.; Raghavachari, K.; Al-Laham, M. A.; Zakrzewski, V. G.; Ortiz, J. V.; Foresman, J. B.; Cioslowski, J.; Stefanov, B. B.; Nanayakkara, A.; Challacombe, M.; Peng, C. Y.; Ayala, P. Y.; Chen, W.; Wong, M. W.; Andres, J. L.; Replogle, E. S.; Gomperts, R.; Martin, R. L.; Fox, D. J.; Binkley, J. S.; Defrees, D. J.; Baker, J.; Stewart, J. P.; Head-Gordon, M.; Gonzalez, C.; Pople, J. A. *Gaussian 94*, revision E.2; Gaussian, Inc.: Pittsburgh, PA, 1995.

(15) Bock, C. W.; Trachtman, M.; Mains, G. J. *J. Phys. Chem.* **1992**, *96*, 3007.

(16) (a) Scott, A. P.; Radom, L. *J. Phys. Chem.* **1996**, *100*, 16502. (b) Rauhut, G.; Pulay, P. *J. Phys. Chem.* **1995**, *99*, 3093.

(17) Timoshkin, A. Y.; Bettinger, H. F.; Schaefer, H. F., III. *J. Am. Chem. Soc.* **1997**, *119*, 5668.

(18) We measured allyldimethylamine in argon (argon:amine ratio of 500:1) to obtain exact IR data for this matrix-isolated molecule. IR (cm^{-1}): 569.0 (vw), 619.5 (vw), 635.5 (vw), 850.0 (w), 855.0 (w), 918.5 (m), 920.0 (m), 923.0 (s), 963.5 (w), 997.5 (w), 1001.0 (w), 1022.5 (w), 1033.0 (m), 1036.5 (s), 1043.5 (m), 1096.5 (w), 1123.0 (w), 1152.0 (vw), 1173.0 (w), 1181.5 (w), 1184.5 (w), 1262.5 (w), 1266.5 (w), 1270.0 (w), 1282.5 (vw), 1350.0 (w), 1405.5 (vw), 1417.0 (w), 1458.5 (m), 1468.5 (m), 1573.0 (vw), 2754.0 (w), 2768.0 (w), 2774.0 (m), 2780.0 (s), 2784.5 (w), 2819.5 (s), 2842.0 (vw), 2850.0 (vw), 2867.5 (vw), 2907.0 (vw), 2953.5 (w), 2965.0 (vw), 2975.0 (vw), 2984.5 (w), 3011.5 (vw), 3081.0 (w).

(19) Kvisle, S.; Rytter, E. *Spectrochim. Acta* **1984**, *40A*, 939.

(20) Ball, D. W.; Pong, R. G. S.; Kafafi, Z. H. *J. Am. Chem. Soc.* **1993**, *115*, 2864.

(21) Jusic, B. S. *J. Mol. Struct. (THEOCHEM)* **1998**, *428*, 61.

(22) Hoffman, B. C.; Sherrill, C. D.; Schaefer, H. F., III. *J. Mol. Struct. (THEOCHEM)* **1996**, *370*, 93.

(23) Selected references: (a) Mitchel, S. A.; Hackett, P. A.; Rayner, D. M.; Humphries, M. R. *J. Chem. Phys.* **1985**, *83*, 5028. (b) Zhang, Y.; Beuermann, T.; Stuke, M. *Appl. Phys.* **1989**, *B48*, 97. (c) Mountziaris, T. J.; Jensen, K. F. *J. Electrochem. Soc.* **1991**, *138*, 2426. (d) Zhang, Y.; Cleaver, W. M.; Stuke, M.; Barron, A. R. *Appl. Phys.* **1992**, *A55*, 261. (e) Naji, O.; Zhang, J.; Kaneko, T.; Jones, T. S.; Neave, J. H.; Joyce, B. A. *J. Cryst. Growth* **1996**, *164*, 58. (f) Nishizawa, J.; Sakuraba, H.; Kurabayashi, T. *J. Vac. Sci. Technol.* **1996**, *B14*, 136.

(24) Himmel, H.-J.; Downs, A. J.; Greene, T. M.; Andrews, L. *J. Chem. Soc., Chem. Commun.* **1999**, 2243.

(25) Bergmann, U.; Reimer, V.; Atakan, B. *Phys. Status Solidi* **1999**, *176*, 719.

(26) Glockling, F.; Strafford, R. G. *J. Chem. Soc. A* **1971**, 1761.

(27) (a) Russell, D. K. *Coord. Chem. Rev.* **1992**, *112*, 131. (b) Russell, D. K. *Chem. Vap. Deposition* **1996**, *2*, 223.

(28) (a) Tsuda, M.; Oikawa, S.; Morishita, M.; Mashita, M. *Jpn. J. Appl. Phys.* **1887**, *26*, L56. (b) Tsuda, M.; Oikawa, S.; Morishita, M.; Mashita, M. *J. Cryst. Growth* **1988**, *91*, 471.

(29) Downs, A. J.; Pulham, C. R. *Adv. Inorg. Chem.* **1994**, *41*, 171.

(30) Köppe, R.; Tacke, M.; Schnöckel, H. *Z. Anorg. Allg. Chem.* **1991**, *605*, 35.

(31) Köppe, R.; Schnöckel, H. *J. Chem. Soc., Dalton Trans.* **1993**, 3393.

(32) Wehmschulte, R. J.; Ellison, J. J.; Ruhlandt-Senge, K.; Power, P. P. *Inorg. Chem.* **1994**, *33*, 6300.

(33) Cowley, A. H.; Gabbaï, F. P.; Isom, H. S.; Carrano, C. J.; Bond, M. R. *Angew. Chem.* **1994**, *106*, 1354; *Angew. Chem., Int. Ed. Engl.* **1994**, *33*, 1253.

(34) Baxter, P. L.; Downs, A. J.; Goode, M. J.; Rankin, D. W. H.; Robertson, H. E. *J. Chem. Soc., Dalton Trans.* **1990**, 2873.

(35) Pulham, C. R.; Downs, A. J.; Goode, M. J.; Rankin, D. W. H.; Robertson, H. E. *J. Am. Chem. Soc.* **1991**, *113*, 5149.

(36) Goode, M. J.; Downs, A. J.; Pulham, C. R.; Rankin, D. W. H.; Robertson, H. E. *J. Chem. Soc., Chem. Commun.* **1988**, 768.

(37) Baxter, P. L.; Downs, A. J.; Rankin, D. W. H.; Robertson, H. E. *J. Chem. Soc., Dalton Trans.* **1985**, 807.

(38) Downs, A. J. Personal communication.

(39) Löwe, A. G.; Hartlieb, A. T.; Brand, J.; Atakan, B.; Kohse-Höinghaus, K. *Combust. Flame* **1999**, *118*, 37.